

Contribution from the Department of Chemistry, The Pennsylvania State University, University Park, Pennsylvania 16802

Crystal and Molecular Structure of a New Hexamolybdate-Cyclophosphazene Complex¹

H. R. ALLCOCK,* E. C. BISSELL, and E. T. SHAWL

Received July 11, 1973

The reaction between molybdenum trioxide and hexakis(dimethylamino)cyclotriphosphazene, $[\text{NP}(\text{NMe}_2)_2]_3$, in water yields yellow-green crystals of the salt $[\text{HN}_3\text{P}_3(\text{NMe}_2)_6]^+[\text{Mo}_6\text{O}_{19}]^{2-}$ (I). Crystals of I are monoclinic with space group $P2_1/c$ and $a = 13.571$ (13), $b = 10.966$ (11), $c = 21.066$ (19) Å, $\beta = 108.36$ (6)°, $Z = 2$. A three-dimensional X-ray structure was determined by Patterson and Fourier methods with refinement by least-squares techniques to a conventional R factor of 0.029. The structure is characterized by the presence of puckered, ring-protonated cyclotriphosphazene structures in which long P-N skeletal bonds (1.663, 1.675 (5) Å) and short skeletal bonds (1.560–1.599 (5) Å) are found in the same ring. The N-P-N skeletal angles are in the range of 109.6–114.5 (3)° and the P-N-P angles are in the range of 126–129 (3)°. The $\text{Mo}_6\text{O}_{19}^{2-}$ ion consists of a slightly distorted cage of six molybdenum atoms located octahedrally around a central oxygen atom, with twelve oxygen atoms disposed in Mo-O-Mo units and one terminal oxygen attached to each molybdenum. The terminal Mo-O bond distances have a range of 1.676–1.678 (5) Å, while the bridge Mo-O bonds have lengths within the range of 1.855–2.005 (4) Å. The central Mo-O bond lengths are in the range of 2.312–2.324 (4) Å. This constitutes the first X-ray structural identification of the $\text{Mo}_6\text{O}_{19}^{2-}$ system.

We report here the reaction of hexakis(dimethylamino)cyclotriphosphazene, $[\text{NP}(\text{NMe}_2)_2]_3$, with molybdenum trioxide, together with the structural characterization of the product, $[\text{HN}_3\text{P}_3(\text{NMe}_2)_6]^+[\text{Mo}_6\text{O}_{19}]^{2-}$ (I), by a single-crystal X-ray diffraction study. The preliminary results of this study have been reported previously.²

The interest in this structure is twofold. First, a number of adducts of acceptor species with phosphazenes have been reported,³ but only for a few of these compounds has the nature of the bonding been characterized adequately. Amino-substituted phosphazenes are known to be strong bases⁴ and either the lone pair of the skeletal nitrogen atoms or the amino substituent could be involved in adduct formation. In the case of $\text{N}_3\text{P}_3\text{Cl}_2(\text{NHP}_r)_4 \cdot \text{HCl}$ it has been demonstrated by an X-ray crystallographic study⁵ that the most basic site is a ring nitrogen atom.

Second, the $\text{Mo}_6\text{O}_{19}^{2-}$ ion is one of the series of discrete isopolymolybdate anions, the structures of which have been the subject of some debate.⁶ The tetrabutylammonium salt of this anion has been isolated and examined by infrared-Raman techniques,^{7,8} and the related isopolyanions $\text{Nb}_6\text{O}_{19}^{8-}$ and $\text{Ta}_6\text{O}_{19}^{8-}$ have been reported,⁹ but there has been no complete X-ray diffraction analysis of this type of structure.

Experimental Section

Synthesis of I. Hexakis(dimethylamino)cyclotriphosphazene, $[\text{NP}(\text{NMe}_2)_2]_3$, was prepared by the interaction of hexachlorocyclotriphosphazene, $(\text{N}_6\text{P}_6\text{Cl}_6)_3$, with excess dimethylamine in boiling chloroform. A mixture of hexakis(dimethylamino)cyclotriphosphazene (5.0 g, 0.0125 mol) and molybdenum trioxide (5.8 g, 0.040 mol) in water (500 ml) was boiled at reflux for 4 hr. During this time, most of the molybdenum trioxide dissolved and a yellow-green solid precipitated. The precipitate was collected, washed with hot *n*-hexane, and then dissolved in dichloromethane. The solution was

then filtered to remove unreacted molybdenum trioxide. The product (6.95 g, 0.0084 mol) was obtained as large yellow-green crystals from a dichloromethane-hexane mixture. The material darkened above 190° and melted with decomposition at 215–216°. It was insoluble in water, 2-butanol, ethyl acetate, tetrahydrofuran, carbon tetrachloride, benzene, and hexane. It was slightly soluble in boiling ethanol and readily soluble in dichloromethane, acetone, acetonitrile, and nitromethane. The correct formulation for this material, as confirmed by the subsequent X-ray structure determination, is $[\text{HN}_3\text{P}_3(\text{NMe}_2)_6]^+[\text{Mo}_6\text{O}_{19}]^{2-}$ (I).

Anal. Calcd for $\text{C}_{24}\text{H}_{74}\text{N}_8\text{O}_{19}\text{Mo}_6$: C, 17.15; H, 4.44; N, 15.00; P, 11.06; Mo, 34.25. Found: C, 17.11, 17.40; H, 4.23, 4.30; N, 14.93; P, 11.50; Mo, 32.00, 32.31.

The following bands were observed in the infrared spectrum (Nujol and Fluorolube mulls) in the region 250–4000 cm^{-1} : 3315 (w), 3075 (w, b), 2990 (vw), 2920 (w), 2875 (m), 2850 (sh), 2802 (w), 2595 (w), 2340 (vw), 2090 (vw), 1940 (vw), 1906 (vw), 1690 (w), 1496 (w, sh), 1476 (m), 1456 (m), 1442 (sh), 1405 (vw), 1312 (m), 1300 (m), 1251 (s), 1211 (m), 1184 (m), 1165 (m), 1144 (sh), 1061 (m), 990 (s), 956 (vs), 913 (s), 858 (w), 796 (s, b), 755 (m), 743 (sh), 723 (vw, sh), 701 (vw), 671 (m), 660 (m), 596 (w, b), 524 (vw), 503 (m), 446 (m), 442 (w, b), 410 (w, sh), 352 (m). The bands at 2595 and 2340 cm^{-1} were assigned to ν_{NH^+} modes. However, an expected ν_{NH^+} band at 2470 cm^{-1} , that is found in $\text{N}_3\text{P}_3(\text{NMe}_2)_6 \cdot \text{HCl}$, was not detected.

The ³¹P nmr spectrum in dichloromethane showed a single resonance at 780 Hz downfield from H_3PO_4 (δ –19.5 ppm, peak width 56 Hz). The ¹H nmr spectrum in dichloromethane showed a complicated pattern of two doublets at τ 7.21 and 7.33 ppm with splittings at 11.8 and 11.4 Hz, respectively. There was a broad peak between each doublet. The signal at 7.21 ppm was the more intense, but an accurate determination of peak areas was not possible. No other resonance was observed in the region down to τ –3.0 ppm. The ³¹P data tentatively suggest that *in solution* the NH proton may be exchanged between different nitrogen atoms. The compound $\text{N}_3\text{P}_3(\text{NMe}_2)_6 \cdot \text{HCl}$ in dichloromethane also showed only one ³¹P peak at δ –20.5 ppm (peak width 42 Hz). The parent compound $\text{N}_3\text{P}_3(\text{NMe}_2)_6$ in the same solvent showed one peak at –25.4 ppm (peak width 40 Hz).

The ¹H nmr spectrum of I is also surprising. The spectrum is more reminiscent of $\text{N}_3\text{P}_3(\text{NMe}_2)_6$ than of $\text{N}_3\text{P}_3(\text{NMe}_2)_6 \cdot \text{HCl}$. The latter showed a sharp peak at τ –0.1 ppm from NH^+ protons, but a comparable peak was not detected in the spectrum of I.

The ultraviolet spectrum of an acetonitrile solution of I showed two absorption maxima at λ 325 nm (ϵ 3080) and λ 257 nm (ϵ 6.20).

Equivalent conductance measurements for acetonitrile solutions of I indicated that it was a strong electrolyte ($\Lambda_e = 106$ at $c = 1.053 \times 10^{-2}$ M, and $\Lambda_e = 142$ at $c = 1.288 \times 10^{-3}$ M).

Collection and Reduction of the X-Ray Data. Single crystals of I for X-ray diffraction studies were grown from a dichloromethane solution to which sufficient *n*-hexane had been added to induce slight turbidity. Crystals deposited quickly as the solvent evaporated. A suitable crystal, 0.26 × 0.26 × 0.16 mm, was chosen; the crystal was transparent and showed uniform extinction under a polarizing microscope. A series of precession photographs indicated that the crystal

(1) This is paper XVI in a series on phosphorus-nitrogen compounds. Part XV: H. R. Allcock, W. J. Cook, and D. P. Mack, *Inorg. Chem.*, **11**, 2584 (1972).

(2) H. R. Allcock, E. C. Bissell, and E. T. Shawl, *J. Amer. Chem. Soc.*, **94**, 8603 (1972).

(3) (a) H. R. Allcock, "Phosphorus-Nitrogen Compounds," Academic Press, New York, N. Y., 1972; (b) H. R. Allcock, *Chem. Rev.*, **72**, 315 (1972).

(4) D. Feakins, R. A. Shaw, P. Watson, and S. N. Nabi, *J. Chem. Soc. A*, 2468 (1969), and references cited therein.

(5) N. V. Mani and A. J. Wagner, *Acta Crystallogr., Sect. B*, **27**, 51 (1971).

(6) H. T. Evans, Jr., *Perspect. Struct. Chem.*, **4**, 1 (1971).

(7) J. Fuchs and K. Jahr, *Z. Naturforsch. B*, **23**, 1380 (1968).

(8) R. Mattes, H. Bierbusse, and J. Fuchs, *Z. Anorg. Allg. Chem.*, **385**, 230 (1971).

(9) I. Lindqvist, *Ark. Kemi*, **5**, 247 (1953); **7**, 49 (1954).

was monoclinic (Laue symmetry $2/m$) and mounted along the 001 direction. The observed systematic absences ($h0l$ for $l = 2n + 1$ and $0k0$ for $k = 2n + 1$) uniquely determine the space group to be $P2_1/c$. The crystal was transferred to a Picker FACS-I diffractometer. Eleven reflections with 2θ (Mo K α) between 16 and 30° were centered on the detector window. The following cell constants and their standard deviations were determined from a least-squares refinement of the setting angles: $a = 13.571$ (13), $b = 10.966$ (11), $c = 21.066$ (19) Å, and $\beta = 108.36$ (6) $^\circ$. $V = 2975.5$, $d_m = 1.88$ g cm $^{-3}$ (by flotation in aqueous zinc chloride solutions), $Z = 2$, $d_c = 1.875$ g cm $^{-3}$, and mol wt (I) 1680.45.

Intensity data were collected using Mo K α radiation with a moving-crystal, moving-counter scan technique; background counts were measured at the beginning and end of the scan range with a stationary crystal and counter. A base scan of 1.2° , a 4-sec background time, and a scan rate of $2^\circ/\text{min}$ were used to $2\theta = 31^\circ$. The base width was then increased to 1.6° with a 10-sec background time. Data between 30.5 and 31° were collected under the two sets of conditions. The scan rate was changed to $1^\circ/\text{min}$ at 36.5° . Reflection data were collected from all the planes hkl and $\bar{h}kl$ to $2\theta = 47.5^\circ$. Because of a malfunction of the Teletype punch unit, the data for two reflections (587 and -2219) were lost and these were eliminated from the data set. Coincidence losses for strong reflections were minimized by the use of a series of calibrated attenuators. During the course of data collection, the intensities of three standard reflections were measured periodically.

The intensities were corrected for average background and then scaled to the standard reflections. The standard deviation of the corrected intensity, $\sigma(I)$, was based on counting statistics. Because the calculated linear absorption coefficient, μ , was 14.4 cm $^{-1}$, no absorption correction was made. Lorentz-polarization corrections were applied and the observed structure factors obtained. The value of σ to be used in the refinement was assigned as follows: $F < 10\sigma(F)$, $\sigma = 1.2$; $F > 33\sigma(F)$, $\sigma = 1.1$; otherwise $\sigma = 1.0$. The equivalent reflections ($hk0$ and $\bar{h}k0$) and the duplicate reflections ($2\theta = 30.5$ – 31°) were averaged. The agreement factor, $R = \sum \mu(\Sigma_i |F_{oi} - \bar{F}_{oi}|) / \sum \mu F_{oi}$, for both sets of reflections was 0.01. Of the 4822 unique reflections collected, 3113 had $I > 2.5\sigma(I)$ and these were used in the subsequent calculations.

Solution and Refinement of the Structure. The atomic scattering factors of Cromer and Waber¹⁰ were used for all nonhydrogen atoms, and those of Stewart, Davidson, and Simpson¹¹ were used for the hydrogen atoms. Anomalous dispersion effects were included with $\Delta f'$ and $\Delta f''$ for Mo and P as given by Cromer.¹² In the least-squares refinement, the function minimized was $\sum w(|F_o| - |F_c|)^2$ with $w = 1/\sigma^2$. The residuals R_1 and R_2 are defined as $R_1 = \Sigma |F_o| - |F_c| / \Sigma |F_o|$ and $R_2 = [\Sigma w(|F_o| - |F_c|)^2 / \Sigma w F_o^2]^{1/2}$.

The three unique molybdenum atoms, clustered about the origin, were located from a map of the three-dimensional Patterson function. After two cycles of least-squares refinement of the positional and isotropic thermal parameters of these atoms with $R_1 = 0.36$, a Fourier synthesis revealed the location of the three phosphorus atoms. Two additional cycles of refinement of the positional and isotropic thermal parameters of these six atoms reduced R_1 to 0.30, and a Fourier synthesis at this point revealed the three nitrogen atoms of the phosphazene ring, the six exocyclic nitrogen atoms, the twelve carbon atoms of the dimethylamino groups, and the nine oxygen atoms. In addition, there was high electron density at the origin in the center of the molybdenum cluster. However, this peak was not assigned at this point. Three more cycles of refinement of the positional and isotropic thermal parameters for all nonhydrogen atoms except (0, 0, 0) gave $R_1 = 0.099$ and $R_2 = 0.109$. A difference Fourier synthesis showed strong residual electron density at the origin; this peak was assigned to an oxygen atom. In addition, residual peaks around the molybdenum and oxygen atoms indicated that anisotropic thermal parameters should be used. Because of the large number of parameters required with the introduction of anisotropic thermal motion, the refinement was divided into two sections with the scale factor, molybdenum, oxygen, phosphorus, and ring nitrogen atoms in one group and the scale factor, phosphorus, nitrogen, and carbon atoms in the second. Each set of parameters was varied in turn. Three cycles of refinement of all nonhydrogen atoms with anisotropic thermal parameters gave $R_1 = 0.043$ and $R_2 = 0.062$.

A difference Fourier synthesis clearly indicated a hydrogen atom attached to one of the ring nitrogen atoms with an electron density of 0.50 e/Å 3 . Eighteen other hydrogen atoms were also located near the amine carbon atoms. At least one hydrogen position was identified at each carbon atom. The hydrogen atoms were positioned according to an idealized model with a C-H distance of 1.00 Å and a tetrahedral geometry around the carbon. Using the nitrogen atom, carbon atom, and one well-located hydrogen atom, the remaining two hydrogen atom positions were generated. These positions were used as a fixed contribution to the structure factor. The isotropic thermal parameter assigned to each hydrogen was the equivalent isotropic thermal parameter of the carbon to which it was bonded. After each full refinement cycle, the hydrogen atom positions were readjusted as necessary to fit the idealized model. Two cycles of refinement with the hydrogen atoms in fixed positions gave $R_1 = 0.035$ and $R_2 = 0.040$.

For the strongest reflections, F_c was systematically larger than F_o indicating that a correction for secondary extinction should be made. The secondary extinction correction of Zachariasen¹³ was incorporated into the least-squares program.¹⁴ Two additional cycles of refinement in which a single extinction parameter, the positional and isotropic thermal parameters of the ring-bonded hydrogen, and the positional and anisotropic parameters of all nonhydrogen atoms were varied gave $R_1 = 0.029$ and $R_2 = 0.031$. The standard deviation of an observation of unit weight based on the 336 variables was 2.11. In the final cycle no parameter changed by more than 0.7 of its standard error. A final difference electron density map had residuals no larger than 0.3 e/Å 3 ; there was some evidence of disorder of the methyl hydrogen atoms around C(1), C(2), C(3), C(4), and C(11). The final value for the secondary extinction parameter was 62 (2) with a corresponding equivalent spherical domain radius of 44 Å. A total of 68 reflections was significantly affected by the extinction correction; the largest percentage change in F_c was 13%. The refined values of the atomic positional and thermal parameters together with the standard deviations, as estimated from the inverse least-squares matrix, are given in Table I. The idealized parameters for the methyl hydrogen atoms are given in Table II. A table of observed and calculated structure factor amplitudes (in electrons $\times 10$) for the 3113 observed reflections is available.¹⁵

All the calculated structure factor amplitudes for the unobserved reflections were small.

Results and Discussion

General Structure of the Complex. Both the conductance data and the X-ray structure determination indicate that compound I is an anion-cation complex of formula $[\text{HN}_3\text{P}_3(\text{NMe}_2)_6]^+ [\text{Mo}_6\text{O}_{19}]^{2-}$. The arrangement of the ions in the unit cell is illustrated in Figure 1.

The unit cell contains two units of formula I, with each unit consisting of a polymolybdate dianion flanked by two cyclöphosphazene cations in an extended arrangement. The proton in each cation unit is linked to a ring nitrogen atom, with each N-H bond pointed toward bridging oxygen atoms in the anion. The outline of each polymolybdate unit is roughly that of an octahedron (Figure 1). The phosphazene rings point toward and are oriented at right angles to opposing edges of this octahedron. The fact that an extended arrangement is preferred raises the possibility that hydrogen bonding between N-H units and bridging oxygen atoms in the polymolybdate may provide a stabilization force. However, the H \cdots O distance is quite long (2.04 (6) Å) for an interaction of this type.

The Hexaisomolybdate Structure. The arrangement of atoms in the polymolybdate dianion is illustrated in Figure 2. The structure consists of six molybdenum atoms located octahedrally around a central oxygen atom. Each molybdenum is then bonded peripherally to neighboring molybdenum atoms through oxygen bridges. One terminal oxygen atom is attached to each molybdenum atom. Alternatively, the

(10) D. T. Cromer and J. T. Waber, *Acta Crystallogr.*, **18**, 104 (1965).

(11) R. F. Stewart, E. T. Davidson, and W. T. Simpson, *J. Chem. Phys.*, **42**, 3175 (1965).

(12) D. T. Cromer, *Acta Crystallogr.*, **18**, 17 (1965).

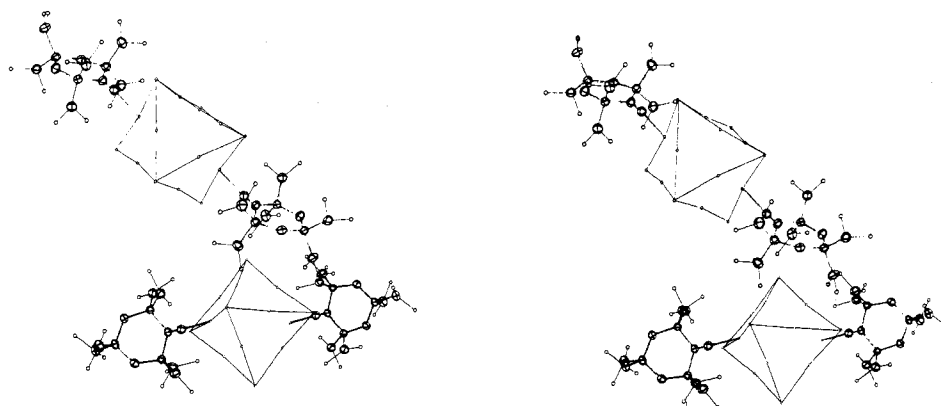
(13) W. H. Zachariasen, *Acta Crystallogr.*, **23**, 558 (1967).

(14) P. Coppens and W. C. Hamilton, *Acta Crystallogr., Sect. A*, **26**, 71 (1970).

(15) See paragraph at end of paper regarding supplementary material.

Table I. Refined Positional and Thermal Parameters for $[\text{HN}_3\text{P}_3[\text{N}(\text{CH}_3)_2]_6]^+ [\text{Mo}_6\text{O}_{19}]^{2-}$

Atom	10^4x	10^4y	10^4z	$10^4\beta_{11}$ (or B)	$10^4\beta_{22}$	$10^4\beta_{33}$	$10^4\beta_{12}$	$10^4\beta_{13}$	$10^4\beta_{23}$
Mo(1)	1783.4 (4)	125.7 (5)	255.1 (3)	31.7 (3)	92.2 (6)	23.7 (2)	-4.9 (4)	7.2 (2)	2.2 (3)
Mo(2)	219.7 (4)	-665.1 (5)	1081.5 (3)	54.2 (4)	88.5 (6)	15.2 (1)	-13.5 (4)	7.4 (2)	3.4 (2)
Mo(3)	-45.1 (4)	2009.4 (5)	340.9 (3)	58.0 (4)	60.6 (5)	23.8 (2)	-0.9 (4)	8.9 (2)	-7.7 (2)
O(1)	3077 (3)	209 (5)	441 (2)	46 (3)	136 (6)	44 (2)	-8 (3)	13 (2)	3 (3)
O(2)	331 (4)	-1221 (5)	1843 (2)	109 (4)	145 (6)	19 (1)	-29 (4)	12 (2)	9 (2)
O(3)	-79 (4)	3432 (4)	624 (2)	104 (4)	78 (4)	37 (2)	3 (4)	19 (2)	-19 (2)
O(4)	1600 (3)	-487 (4)	1077 (2)	49 (3)	93 (4)	21 (1)	-4 (3)	1 (1)	7 (2)
O(5)	1285 (3)	747 (4)	-639 (2)	53 (3)	99 (4)	24 (1)	-14 (3)	19 (1)	3 (2)
O(6)	1406 (3)	1700 (4)	536 (2)	55 (3)	77 (4)	24 (1)	-17 (3)	8 (1)	-7 (2)
O(7)	-1487 (3)	1482 (4)	98 (2)	53 (3)	91 (4)	31 (1)	6 (3)	14 (2)	-5 (2)
O(8)	206 (3)	-2191 (4)	562 (2)	63 (3)	70 (4)	24 (1)	-4 (3)	7 (2)	5 (2)
O(9)	88 (3)	1010 (4)	1161 (2)	81 (3)	87 (4)	23 (1)	-15 (3)	17 (2)	-14 (2)
O(10)	0	0	0	37 (3)	58 (5)	16 (1)	0 (3)	8 (2)	-1 (2)
P(1)	2826 (1)	1381 (1)	4021 (1)	50 (1)	50 (1)	19 (1)	3 (1)	1 (1)	1 (1)
P(2)	4466 (1)	1651 (1)	3479 (1)	40 (1)	65 (1)	18 (1)	6 (1)	7 (1)	-7 (1)
P(3)	3021 (1)	3613 (1)	3258 (1)	43 (1)	53 (1)	16 (1)	1 (1)	8 (1)	1 (1)
N(1)	2531 (4)	2817 (4)	3760 (2)	50 (3)	57 (5)	21 (1)	6 (3)	15 (2)	0 (2)
N(2)	3899 (3)	1015 (4)	3951 (2)	55 (3)	62 (5)	21 (1)	4 (3)	10 (2)	-3 (2)
N(3)	4006 (3)	2956 (4)	3195 (2)	53 (3)	72 (5)	23 (1)	12 (3)	14 (2)	4 (2)
N(4)	1891 (4)	494 (4)	3584 (3)	58 (4)	56 (5)	34 (2)	-3 (3)	11 (2)	3 (2)
N(5)	2822 (4)	1362 (5)	4791 (3)	77 (4)	90 (6)	24 (2)	-2 (4)	17 (2)	6 (2)
N(6)	4471 (4)	819 (5)	2825 (2)	70 (4)	103 (6)	21 (1)	16 (4)	13 (2)	-12 (2)
N(7)	5712 (4)	1711 (5)	3927 (2)	45 (3)	93 (6)	25 (2)	7 (3)	9 (2)	-11 (2)
N(8)	3313 (4)	4993 (5)	3535 (3)	65 (4)	63 (5)	31 (2)	1 (4)	18 (2)	-4 (2)
N(9)	2054 (4)	3819 (5)	2566 (2)	53 (3)	103 (6)	24 (2)	2 (4)	6 (2)	13 (2)
C(1)	783 (5)	783 (7)	3455 (5)	55 (5)	84 (8)	65 (4)	-9 (5)	12 (3)	4 (4)
C(2)	2075 (6)	-778 (7)	3459 (4)	77 (6)	83 (7)	51 (3)	-8 (5)	15 (3)	-19 (4)
C(3)	2217 (7)	542 (7)	5061 (4)	160 (9)	91 (8)	44 (3)	15 (7)	63 (4)	17 (4)
C(4)	3658 (6)	1976 (8)	5297 (3)	95 (6)	161 (10)	23 (2)	-5 (7)	13 (3)	3 (4)
C(5)	3721 (7)	1016 (9)	2183 (4)	126 (8)	217 (14)	25 (2)	52 (9)	0 (3)	-32 (5)
C(6)	4851 (6)	-426 (7)	2950 (4)	113 (7)	108 (9)	42 (3)	26 (6)	26 (4)	-23 (4)
C(7)	6422 (5)	2246 (7)	3601 (4)	61 (5)	104 (8)	39 (2)	-5 (5)	20 (3)	0 (4)
C(8)	5977 (5)	2035 (7)	4633 (3)	64 (5)	134 (9)	27 (2)	14 (6)	0 (3)	-11 (4)
C(9)	4330 (6)	5282 (8)	3993 (5)	97 (7)	112 (9)	51 (3)	-25 (6)	8 (4)	-31 (4)
C(10)	2519 (7)	5915 (6)	3511 (5)	122 (7)	59 (7)	65 (4)	-2 (6)	53 (4)	-7 (4)
C(11)	1304 (6)	2849 (8)	2285 (3)	89 (6)	142 (10)	25 (2)	-20 (6)	-3 (3)	-2 (4)
C(12)	2234 (6)	4607 (9)	2054 (4)	77 (6)	231 (14)	30 (2)	-12 (7)	5 (3)	41 (5)
H(N1)	2123 (43)	3197 (52)	3919 (28)	3.3 (14)					

Figure 1. Stereoscopic view of the unit cell showing the disposition of the two $[\text{HN}_3\text{P}_3(\text{NMe}_2)_6]^+ [\text{Mo}_6\text{O}_{19}]^{2-}$ arrays.

structure can be visualized as formed from six MoO_6 octahedra that have condensed so that they all share a common vertex. Bond angles and bond lengths are shown in Table III, with atom designations that correspond to those shown in structure II.

This structure determination constitutes the first X-ray crystallographic identification of the $\text{Mo}_6\text{O}_{19}^{2-}$ species, a result that is of some interest in view of recent discussions related to the structures of isopoly and heteropoly anions.¹⁶⁻¹⁸ The structure of $\text{Mo}_6\text{O}_{19}^{2-}$ corresponds to the one suggested by Kepert.¹⁸ Infrared evidence for the existence of the

$\text{Mo}_6\text{O}_{19}^{2-}$ ion has been reported earlier¹⁶ and an optical spectrum believed to originate from the same ion was described by So and Pope.¹⁶ This spectrum matches the one recorded for I (see Experimental Section). In broader terms the structure of the $\text{Mo}_6\text{O}_{19}^{2-}$ ion resembles that of the $\text{W}_6\text{O}_{19}^{2-}$ ion.^{6,19,20}

One curious feature of the $\text{Mo}_6\text{O}_{19}^{2-}$ structure is a slight distortion of the octahedron that involves the bridging bonds on the surface of the cage. This distortion is illustrated by the data in Table III. The molybdenum octahedron surround-

(16) H. So and M. T. Pope, *Inorg. Chem.*, 11, 1441 (1972).(17) M. T. Pope, *Inorg. Chem.*, 11, 1973 (1972).(18) D. L. Kepert, *Inorg. Chem.*, 8, 1556 (1969).(19) K. F. Jahr, J. Fuchs, and R. Oberhauser, *Chem. Ber.*, 101, 477 (1968).(20) G. Henning and A. Hullen, *Z. Kristallogr., Kristallgeometrie, Kristallphys., Kristallchem.*, 130, 162 (1969).

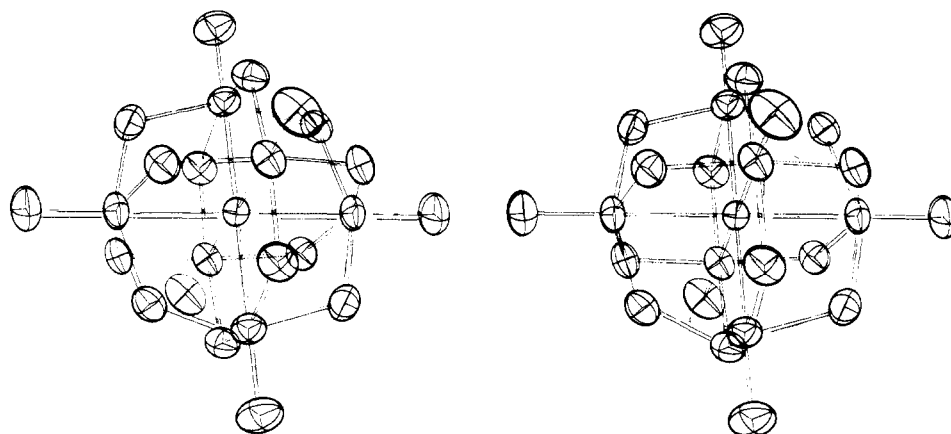


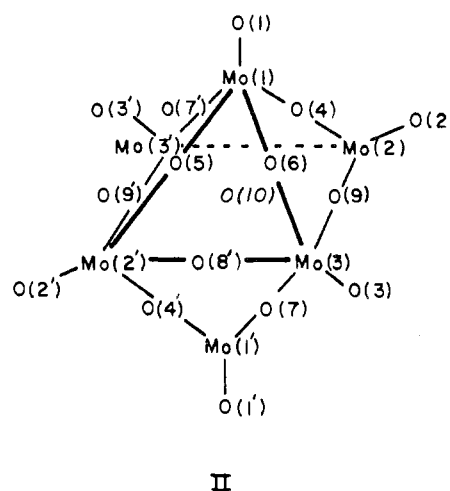
Figure 2. Stereoscopic view of the hexaisomolybdate dianion. An oxygen atom occupies the center, surrounded by six molybdenum atoms in an octahedral arrangement.

Table II. Idealized Hydrogen Atom Positional Parameters

Atom	10^4x	10^4y	10^4z	$B, \text{Å}^2$
H(1)	470	177	3690	6.252
H(2)	716	1621	3625	6.252
H(3)	412	748	2963	6.252
H(4)	1820	-1312	3759	5.879
H(5)	1697	-982	2981	5.879
H(6)	2836	-913	3551	5.879
H(7)	2665	207	5498	6.486
H(8)	1621	997	5131	6.486
H(9)	1946	-144	4740	6.486
H(10)	4040	2522	5074	5.946
H(11)	3361	2474	5591	5.946
H(12)	4147	1356	5573	5.946
H(13)	3456	1872	2155	8.040
H(14)	4052	880	1827	8.040
H(15)	3130	434	2118	8.040
H(16)	4995	-751	2545	6.343
H(17)	5504	-437	3339	6.343
H(18)	4315	-945	3053	6.343
H(19)	7156	2063	3873	5.028
H(20)	6275	1890	3144	5.028
H(21)	6318	3150	3565	5.028
H(22)	6747	1981	4847	5.284
H(23)	5742	2887	4674	5.284
H(24)	5626	1460	4861	5.284
H(25)	4824	4609	3987	7.018
H(26)	4583	6062	3853	7.018
H(27)	4285	5373	4455	7.018
H(28)	1846	5667	3176	6.481
H(29)	2427	5988	3962	6.481
H(30)	2742	6720	3379	6.481
H(31)	1551	2072	2532	5.976
H(32)	615	3076	2329	5.976
H(33)	1234	2736	1802	5.976
H(34)	2886	5086	2252	7.276
H(35)	2305	4095	1678	7.276
H(36)	1635	5178	1881	7.276

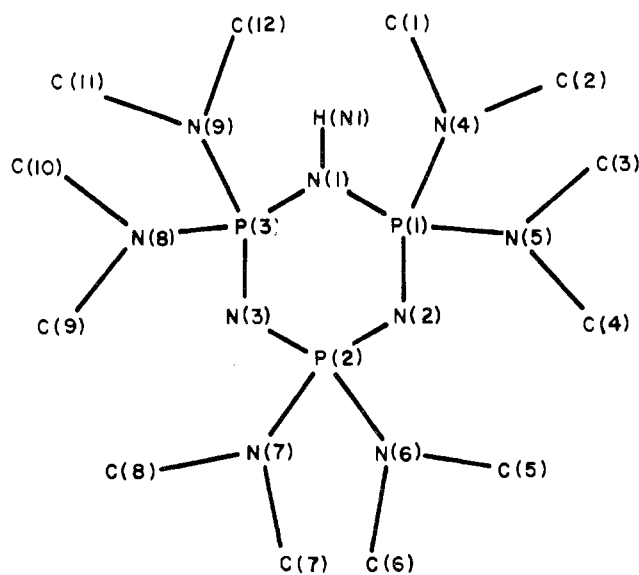
ing the central oxygen is essentially regular, but the bridging oxygen atoms are not exactly equidistant from the flanking molybdenum atoms. Specifically Mo(2)-O(4) (1.886 Å), Mo(2)-O(9) (1.859 Å), Mo(3)-O(8) (1.855 Å), and symmetry-related bonds are shorter than the other bridging bonds (which are in the range of 1.906-2.005 Å) (the designation of the atoms is illustrated in structure II). A similar distortion has been reported for the $V_{10}O_{28}^{2-}$ ion.²¹

The terminal Mo-O bonds are shorter (1.677 Å) than the average bridging Mo-O bonds (mean value 1.928 Å) as expected, whereas the central Mo-O bonds are longer (2.319 Å).



II

The Cyclophosphazene Structure. Bond distances and angles for the cyclophosphazene structure are listed in Table IV, with atom designations that correspond to those in structure III. Perhaps the most interesting feature of the cyclo-



III

phosphazene structure is the unambiguous location of a proton linked directly to a ring nitrogen (Figure 1 and structure

(21) A. G. Swallow, F. R. Ahmed, and W. H. Barnes, *Acta Crystallogr.*, 21, 397 (1966).

Table III. Bond Distances and Angles in Isopolymolybdate Unit^a

Atoms	Distance, Å	Atoms	Distance, Å
Terminal		Bridging	
Mo(1)-O(1)	1.676 (4)	Mo(1)-O(4)	1.944 (4)
Mo(2)-O(2)	1.678 (4)	Mo(1)-O(5)	1.914 (4)
Mo(3)-O(3)	1.676 (5)	Mo(1)-O(6)	1.945 (4)
Central		Mo(1)-O(7)	1.906 (4)
Mo(1)-O(10)	2.312 (4)	Mo(2)-O(4)	1.886 (4)
Mo(2)-O(10)	2.320 (4)	Mo(2)-O(5)	1.961 (4)
Mo(3)-O(10)	2.324 (4)	Mo(2)-O(8)	1.996 (4)
		Mo(2)-O(9)	1.859 (4)
		Mo(3)-O(6)	1.911 (4)
		Mo(3)-O(7)	1.948 (4)
		Mo(3)-O(8)	1.855 (4)
		Mo(3)-O(9)	2.005 (4)
Atoms	Angle, deg	Atoms	Angle, deg
Terminal-Bridging		Terminal-Central	
O(1)-Mo(1)-O(4)	103.3 (2)	O(1)-Mo(1)-O(10)	179.7 (2)
O(1)-Mo(1)-O(5)	103.3 (2)	O(2)-Mo(2)-O(10)	176.4 (2)
O(1)-Mo(1)-O(6)	103.7 (2)	O(3)-Mo(3)-O(10)	177.1 (2)
O(1)-Mo(1)-O(7)	102.6 (2)	Bridging-Bridging	
O(2)-Mo(2)-O(4)	104.6 (2)	O(4)-Mo(1)-O(5)	153.4 (2)
O(2)-Mo(2)-O(5)	101.8 (2)	O(4)-Mo(1)-O(6)	85.2 (2)
O(2)-Mo(2)-O(8)	101.7 (2)	O(4)-Mo(1)-O(7)	87.6 (2)
O(2)-Mo(2)-O(9)	104.8 (2)	O(5)-Mo(1)-O(6)	86.5 (2)
O(3)-Mo(3)-O(6)	103.4 (2)	O(5)-Mo(1)-O(7)	88.8 (2)
O(3)-Mo(3)-O(7)	103.4 (2)	O(6)-Mo(1)-O(7)	153.6 (2)
O(3)-Mo(3)-O(8)	105.0 (2)	O(4)-Mo(2)-O(5)	152.7 (2)
O(3)-Mo(3)-O(9)	101.9 (2)	O(4)-Mo(2)-O(8)	85.5 (2)
Bridging-Central		O(4)-Mo(2)-O(9)	91.3 (2)
O(4)-Mo(1)-O(10)	76.6 (2)	O(5)-Mo(2)-O(8)	82.7 (2)
O(5)-Mo(1)-O(10)	76.9 (2)	O(5)-Mo(2)-O(9)	88.4 (2)
O(6)-Mo(1)-O(10)	76.5 (2)	O(8)-Mo(2)-O(9)	153.3 (2)
O(7)-Mo(1)-O(10)	77.1 (2)	O(6)-Mo(3)-O(7)	152.3 (2)
O(4)-Mo(2)-O(10)	77.5 (2)	O(6)-Mo(3)-O(8)	91.1 (2)
O(5)-Mo(2)-O(10)	75.8 (2)	O(6)-Mo(3)-O(9)	84.9 (2)
O(8)-Mo(2)-O(10)	75.5 (2)	O(7)-Mo(3)-O(8)	88.8 (2)
O(9)-Mo(2)-O(10)	77.9 (2)	O(7)-Mo(3)-O(9)	82.8 (2)
O(6)-Mo(3)-O(10)	76.8 (2)	O(8)-Mo(3)-O(9)	153.0 (2)
O(7)-Mo(3)-O(10)	76.1 (2)		
O(8)-Mo(3)-O(10)	77.9 (2)		
O(9)-Mo(3)-O(10)	75.2 (2)		

^a The atoms are labeled according to the scheme shown in structure II.

III). This confirms what has been suspected for a number of years,²²⁻²⁴ that the ring nitrogen atoms in aminocyclophosphazenes can be more basic than the nitrogen atoms of the amino-substituted groups. Ring protonation has also been confirmed in an X-ray crystallographic study of N₃P₃Cl₂(NHP_r)₄·HCl (II) by Mani and Wagner,⁵ but in that structure the N-H bond distance was 0.2 Å longer than in I.

The phosphazene rings are puckered in a distorted chair conformation (Tables V and VI). The bonds which flank the protonated nitrogen atom are longer (1.663, 1.675 Å) than the other skeletal P-N bonds (1.560-1.599 Å) and this is consistent with the decrease in π' character in this region of the molecule. Those skeletal bonds which involve non-protonated nitrogen atoms are comparable in length to those found in other dimethylaminocyclophosphazenes.^{25,26} The

(22) D. Feakins, W. A. Last, and R. A. Shaw, *Chem. Ind. (London)*, 510 (1962).

(23) T. Moeller and S. G. Kokalis, *J. Inorg. Nucl. Chem.*, **25**, 875 (1963).

(24) D. Feakins, W. A. Last, and R. A. Shaw, *J. Chem. Soc.*, 4464 (1964).

(25) G. J. Bullen, *J. Chem. Soc.*, 3193 (1962).

(26) A. J. Wagner and A. Vos, *Acta Crystallogr., Sect. B*, **24**, 1423 (1968).

Table IV. Bond Distances and Angles in Cyclophosphazene Unit^{a,b}

Atoms	Distance, Å	Atoms	Angle, deg
Ring Distances		Ring Angles	
P(1)-N(1)	1.675 (5)	N(1)-P(1)-N(2)	110.1 (2)
P(1)-N(2)	1.562 (5)	P(1)-N(2)-P(2)	126.4 (3)
P(2)-N(2)	1.596 (5)	N(2)-P(2)-N(3)	114.5 (2)
P(2)-N(3)	1.599 (5)	P(2)-N(3)-P(3)	128.8 (3)
P(3)-N(3)	1.560 (5)	N(3)-P(3)-N(1)	109.6 (3)
P(3)-N(1)	1.663 (5)	P(3)-N(1)-P(1)	126.9 (3)
Exocyclic Distances		P(1)-N(1)-H(N1)	117 (4)
P(1)-N(4)	1.634 (5)	P(3)-N(1)-H(N1)	116 (3)
P(1)-N(5)	1.622 (5)	Exocyclic Angles	
P(2)-N(6)	1.655 (5)	N(4)-P(1)-N(5)	108.0 (3)
P(2)-N(7)	1.658 (5)	N(6)-P(2)-N(7)	103.0 (3)
P(3)-N(8)	1.626 (5)	N(8)-P(3)-N(9)	103.1 (3)
P(3)-N(9)	1.641 (5)	N(4)-P(1)-N(1)	108.2 (3)
N(1)-H(N1)	0.84 (6) ^c	N(4)-P(1)-N(2)	112.0 (3)
N(4)-C(1)	1.477 (8)	N(5)-P(1)-N(1)	105.4 (3)
N(4)-C(2)	1.455 (9)	N(5)-P(1)-N(2)	112.9 (3)
N(5)-C(3)	1.450 (10)	N(6)-P(2)-N(2)	114.0 (3)
N(5)-C(4)	1.455 (9)	N(6)-P(2)-N(3)	106.6 (3)
N(6)-C(5)	1.430 (9)	N(7)-P(2)-N(2)	105.6 (3)
N(6)-C(6)	1.453 (10)	N(7)-P(2)-N(3)	112.7 (3)
N(7)-C(7)	1.470 (8)	N(8)-P(3)-N(1)	111.2 (3)
N(7)-C(8)	1.459 (8)	N(8)-P(3)-N(3)	110.0 (3)
N(8)-C(9)	1.448 (10)	N(9)-P(3)-N(1)	105.6 (3)
N(8)-C(10)	1.467 (9)	N(9)-P(3)-N(3)	117.1 (3)
N(9)-C(11)	1.462 (10)	C(1)-N(4)-C(2)	113.3 (5)
N(9)-C(12)	1.462 (10)	C(1)-N(4)-P(1)	122.7 (5)
Hydrogen Bond		C(2)-N(4)-P(1)	121.7 (4)
H(N1)-O(5)	2.04 (6)	C(3)-N(5)-C(4)	114.0 (6)
		C(3)-N(5)-P(1)	125.6 (5)
		C(4)-N(5)-P(1)	118.6 (5)
		C(5)-N(6)-C(6)	114.8 (6)
		C(5)-N(6)-P(2)	121.1 (5)
		C(6)-N(6)-P(2)	117.5 (5)
		C(7)-N(7)-C(8)	113.0 (5)
		C(7)-N(7)-P(2)	116.8 (4)
		C(8)-N(7)-P(2)	118.0 (4)
		C(9)-N(8)-C(10)	114.1 (6)
		C(9)-N(8)-P(3)	121.1 (5)
		C(10)-N(8)-P(3)	122.4 (5)
		C(11)-N(9)-C(12)	112.8 (5)
		C(11)-N(9)-P(3)	121.3 (5)
		C(12)-N(9)-P(3)	117.6 (4)
Hydrogen Bond			
		N(1)-H(N1)-O(5)	173 (5)

^a For the exocyclic P-N bonds $\chi^2 = 44$, $\rho < 0.01$. Therefore the bond distances are significantly different. ^b For the N-C bonds, $\chi^2 = 19.8$, $\rho = 0.05$, and the distances are considered to be equal (mean value is 1.457 Å). ^c Bond distance when corrected for thermal motion is 0.89 Å (assuming independent motion or H(N1) riding on N(1)).

Table V. Distances of the Phosphazene Ring Atoms from the Least-Squares Plane^{a,b}

HN ₃ P ₃ (NMe ₂) ₆ ⁺ Plane Equation: 0.329x + 0.448y + 0.831z = 7.86 ^c			
Atoms	Distance, Å	Atoms	Distance, Å
P(1)	0.111 (2)	N(1)	-0.085 (5)
P(2)	0.028 (2)	N(2)	-0.087 (5)
P(3)	0.030 (1)	N(3)	0.003 (5)

^a $\chi^2 = 7121$. ^b The nonplanar ring occupies a distorted chair conformation. ^c The coordinates for the plane are given in an orthogonal coordinate system defined by the a, b, and c* axes of the cell.

bonds between phosphorus and the nitrogen atoms of the substituent groups are longer (1.622-1.641 Å) than those of the nonprotonated ring units, but shorter than those of the

Table VI. Torsional Angles within the Phosphazene Ring

Bonds	Angle, deg	Bonds	Angle, deg
P(1)-N(1)-P(3)-N(3)	-13.9	N(3)-P(2)-N(2)-P(1)	15.1
N(1)-P(3)-N(3)-P(2)	6.6	P(2)-N(2)-P(1)-N(1)	-20.5
P(3)-N(3)-P(2)-N(2)	-7.0	N(2)-P(1)-N(1)-P(3)	20.4

protonated segment. This could suggest some $d_{\pi}-p_{\pi}$ bonding involvement in the exocyclic P-N bonds. Of special interest is the angle P(3)-N(1)H-P(1), which is 126.9° . This can be compared to the 123° angle reported for a cyclotriphosphazene^{3,5} and the 132° angle reported for the P-NH-P unit in II.⁵ Apparently the bond angle at nitrogen is especially flexible and it responds more to the demands of the ring geometry as a whole than to the hybridization requirements at a particular site. The endocyclic ring angles at phosphorus are in the range of $109.6-114.5^{\circ}$, values that are unusually narrow compared with many other cyclotriphosphazenes. Similar effects were reported for II.⁵ This could be a consequence of reduced ring π bonding. The exocyclic N-P-N bond angles, which fall within the range $103.0-108.0^{\circ}$,

are normal for cyclotriphosphazenes,²⁷ and, as expected, the N(exo)-P-N(exo) planes are oriented approximately at right angles to the adjacent N(ring)-P-N(ring) plane.

Acknowledgment. We thank the donors of the Petroleum Research Fund, administered by the American Chemical Society, for the support of most of this work.

Registry No. $[\text{HN}_3\text{P}_3(\text{NMe}_2)_6]_2[\text{Mo}_6\text{O}_{19}]$, 37369-90-7; MoO_3 , 1313-27-5.

Supplementary Material Available. A listing of observed and calculated structure factor amplitudes will appear following these pages in the microfilm edition of this volume of the journal. Photocopies of the supplementary material from this paper only or microfiche (105×148 mm, 20X reduction, negatives) containing all of the supplementary material for the papers in this issue may be obtained from the Journals Department, American Chemical Society, 1155 16th St., N.W., Washington, D. C. 20036. Remit check or money order for \$4.00 for photocopy or \$2.00 for microfiche, referring to code number INORG-73-2963.

(27) Reference 3a, Appendix I.

Contribution from the Department of Chemistry,
California State University, San Diego, California 92115

Pyrolysis of Halodisilanes and the Formation and Insertion Reactions of Chlorosilylene and Fluorosilylene

R. L. JENKINS, A. J. VANDERWIELEN, S. P. RUIS, S. R. GIRD, and M. A. RING*

Received March 1, 1973

The pyrolysis of Si_2F_6 , FSi_2H_5 , ClSi_2H_5 , $1,1\text{-F}_2\text{Si}_2\text{H}_4$, $1,1\text{-Cl}_2\text{Si}_2\text{H}_4$, and $((\text{CH}_3)_2\text{SiHCl})_2$ was examined as neat and in the presence of other silanes. The results from these pyrolyses demonstrated that all six disilanes decomposed into a silylene and a silane. In $((\text{CH}_3)_2\text{SiHCl})_2$ the relative rate of the 1,2 hydrogen shift compared to the 1,2 chlorine shift was 4.4 ± 0.4 . 1,2 halogen shifts were not observed in $1,1\text{-F}_2\text{Si}_2\text{H}_4$ or $1,1\text{-Cl}_2\text{Si}_2\text{H}_4$. The insertions of silylenes into the silicon-hydrogen bonds in ethylsilane were examined. The product ratios coupled with assumptions of the half-lives of the silylenes led to the following order for silylene insertion rates: $\text{SiH}_2 > \text{ClSiH} > \text{FSiH} \gg \text{Cl}_2\text{Si}, \text{F}_2\text{Si}$.

Introduction

It was suggested that $\text{Si}_2(\text{CH}_3)_5\text{H}$ thermally decomposed by a 1,2 hydrogen shift to form $\text{HSi}(\text{CH}_3)_3$ and $\text{Si}(\text{CH}_3)_2$.¹ It has now been demonstrated that Si_2H_6 ,^{2,3} $\text{CH}_3\text{Si}_2\text{H}_5$,⁴ and $1,2\text{-(CH}_3)_2\text{Si}_2\text{H}_4$ ⁴ decompose via 1,2 hydrogen shifts producing a silane and a silylene. Methoxydisilanes also decompose into a silylene and a silane via a 1,2 methoxy shift.^{5,6} In the above reactions, the silylenes have been chemically trapped.

It has also been suggested that Si_2F_6 decomposes similarly via a 1,2 fluorine shift.⁷ Dichlorosilylene has been generated and chemically trapped in the flow pyrolysis of Si_2Cl_6 and C_2H_2 .⁸

We have examined the pyrolysis (under flow conditions with low-temperature removal of products) of a number of substituted disilanes in order to determine the following: (i) the relative rate of a 1,2 hydrogen shift vs. a 1,2 chlorine shift when both hydrogen and chlorine are in the same environment; (ii) the effects of environment on the rates of 1,2 hydrogen shifts; (iii) the relative rates of SiF_2 , SiCl_2 , HSiF , HSiCl , and SiH_2 insertion into silicon-hydrogen bonds.

Experimental Section

The silanes and alkylsilanes used were prepared by the reduction of the corresponding chloro compounds with LiAlH_4 or LiAlD_4 . Hexafluorodisilane was prepared by reaction of Si_2Cl_6 with SbF_3 .⁹ 1,1-Dichlorodisilane was obtained from the reaction of Si_2H_6 with HCl over Al_2Cl_6 ,¹⁰ while $1,1\text{-F}_2\text{Si}_2\text{H}_4$ was obtained from the reaction of $1,1\text{-Cl}_2\text{Si}_2\text{H}_4$ with SbF_3 .¹¹ Chlorodisilane and FSi_2H_5 were prepared by chlorination of Si_2H_6 ¹⁰ followed by fluorination of ClSi_2H_5 with SbF_3 in a flow reactor. The new compound 1,2-dichloro-1,2-dimethyldisilane, $\text{sym-Cl}_2\text{Si}_2\text{H}_2(\text{CH}_3)_2$, was prepared by the reaction of $1,2\text{-(CH}_3)_2\text{Si}_2\text{H}_4$ with AgCl in a flow reactor as previously described¹² with the cold trap at -45° and the reactor at 25° .

(1) H. Sakurai, A. Hosomi, and M. Kumada, *Chem. Commun.*, 5 (1969).

(2) P. Estacio, M. D. Sefcik, E. K. Chan, and M. A. Ring, *Inorg. Chem.*, 9, 1068 (1970).

(3) M. Bowery and J. H. Purnell, *J. Amer. Chem. Soc.*, 92, 2594 (1970).

(4) R. B. Baird, M. D. Sefcik and M. A. Ring, *Inorg. Chem.*, 10, 883 (1971).

(5) W. H. Atwell and D. R. Weyenberg, *J. Organometal. Chem.*, 5, 594 (1966).

(6) W. H. Atwell and D. R. Weyenberg, *J. Amer. Chem. Soc.*, 90, 3438 (1968).

(7) M. Schmeisser and K. P. Ehlers, *Angew. Chem.*, 76, 781 (1964).

(8) E. A. Chernyshev, N. G. Kamalenkov, and S. A. Bashkerova, *Zh. Obshch. Khim.*, 41, 1175 (1971).

(9) H. J. Emeleus and A. G. Maddock, *J. Chem. Soc.*, 293 (1944).

(10) R. P. Hollandsworth and M. A. Ring, *Inorg. Chem.*, 7, 1635 (1968).

(11) J. E. Drake and N. Goddard, *J. Chem. Soc. A*, 2587 (1970).